

Pattern selection and the effect of group velocity on interacting oscillatory and stationary instabilities

D. Walgraef*

Departament de Física, Universitat de les Illes Balears, E-07071 Palma de Mallorca, Spain

(Received 29 August 1996)

The effect of mean flows on pattern stability in systems where oscillatory instabilities of the Hopf type interact with stationary ones is investigated. In particular, it is shown that pattern selection may be strongly modified when the absolute instability threshold of the trivial uniform steady state is rejected beyond the stationary instability. The effect of spatially distributed noise including the competition between noise sustained and dynamically sustained structures is also discussed. [S1063-651X(97)01006-4]

PACS number(s): 47.20.Ky, 05.40.+j, 43.50.+y, 47.50.+d

I. INTRODUCTION

Several physicochemical systems driven out of equilibrium present oscillatory instabilities or Hopf bifurcations leading to the formation of spatiotemporal wave patterns. Celebrated examples are Rayleigh-Bénard instabilities in binary fluids [1], electrohydrodynamic instabilities in nematic liquid crystals [2], or convective instabilities in Taylor-Couette systems [3]. Close to the instability, the systems dynamics may be reduced, in one-dimensional geometries, to coupled complex Ginzburg-Landau equations that describe the evolution of the amplitude of counterpropagating waves that may appear beyond the bifurcation point [4]. The coefficients of these equations have been evaluated by means of analytical and numerical techniques for binary fluid convection for different separation ratios, Prandtl numbers, and Lewis numbers [5] and for polymeric fluid convection for different fluid characteristics [6]. From the values of these kinetic coefficients of these equations, which have been derived directly from the Navier-Stokes equations, it appears that in binary fluid convection the selected pattern should correspond to traveling waves, while in viscoelastic convection there is a wide range of parameters where the selected stable patterns should correspond to standing waves. Furthermore, in the latter case, the amplitude and phase stability of these standing waves versus extended perturbations have been computed for a series of typical values of the parameters corresponding to polymeric solutions ranging from Jeffreys to Maxwellian [7].

However, these Ginzburg-Landau equations contain mean flow terms induced by group velocities whose importance varies according to the fluid under consideration. As a result, one also has to study the convective and absolute stability of the wave patterns. Let me recall that when the reference state is convectively unstable, localized perturbations are driven by the mean flow in such a way that they grow in the moving reference frame, but decay at any fixed location. On the contrary, in the absolute instability regime, localized perturba-

tions grow at any fixed location [8]. As a result, the behavior of the system is qualitatively very different in both regimes. In the convectively unstable regime, a deterministic system cannot develop the expected wave patterns, except in particular experimental setups (e.g., in annular containers or in the presence of reflecting boundaries), while in a stochastic system noise is spatially amplified and gives rise to noise-sustained structures [9]. On the contrary, in the absolutely unstable regime, waves are intrinsically sustained by the deterministic dynamics, which provides the relevant selection and stability criteria [10,11]. Hence the concepts of convective and absolute instability are essential to understand the behavior of nonlinear wave patterns and their stability [9,12].

Noise-sustained wave patterns have been widely studied, first, in systems where single or counterpropagating traveling waves are preferred and, more recently, in systems where it is standing waves that are the preferred structures [9,13–18]. In particular, in the latter case, it has been shown that in deterministic systems transitions from the conduction state to traveling waves and finally to standing waves occur at thresholds that depend on the group velocity, while in stochastic systems standing waves are sustained by noise in all the parameter range beyond the Hopf bifurcation [18].

Besides the oscillatory instabilities, many of these systems also present stationary instabilities leading to steady spatial patterns. Which type of convection appears first, oscillatory or stationary, is determined, in polymeric fluids, by their rheological parameters. In particular, at fixed Prandtl numbers, it is the stress relaxation time that fixes the relative position of each instability threshold. Hence, in the case where oscillatory instability appears first, the corresponding absolute instability may nevertheless be rejected beyond the stationary instability if the group velocity is sufficiently large, such as in Maxwell fluids. In this case, the difference between deterministic and stochastic systems should be qualitative in nature. Effectively, in deterministic systems, stationary patterns should develop first, even though the Hopf bifurcation is the first to appear, while in stochastic systems, standing waves should be sustained by noise in beyond the Hopf bifurcation.

To describe this situation, one needs to consider coupled amplitude equations for interacting oscillatory and steady modes. The aim of this paper is to achieve a qualitative understanding of the behavior of such dynamical systems for

*Permanent address: Center for Nonlinear Phenomena and Complex Systems, Free University of Brussels, Case Postale 231, Boulevard du Triomphe, B-1050 Brussels, Belgium.

arbitrary values of the cross-coupling coefficients and of the group velocity and to analyze the effect of these parameters on the pattern selection, either in deterministic and stochastic systems.

The paper is organized as follows. In Sec. II, amplitude equations for interacting oscillatory and stationary modes are presented in the general case. In Sec. III, convective and absolute instability thresholds are determined for the different ground states when the cross coupling between counter-propagating waves sustains traveling waves or standing waves. The resulting pattern selection is analyzed for deterministic systems in Sec. IV and for stochastic systems in Sec. V. Numerical checks are presented in Sec. VI and conclusions are drawn in Sec. VII.

II. AMPLITUDE EQUATIONS FOR INTERACTING OSCILLATORY AND STATIONARY INSTABILITIES

Let me consider a driven physicochemical system where an oscillatory instability, say, a Hopf bifurcation with broken spatial symmetry, and a stationary pattern forming instability are close together. In their vicinity, the order-parameter-like variable may be written, in one-dimensional horizontal geometries, as

$$\vec{u}(\vec{r}, t) = [\vec{u}_0(z)(A(X, T)e^{i(k_c x + \omega_c t)} + B(X, T)e^{-i(k_c x - \omega_c t)} + \vec{u}_s(z)R(X, T)e^{ik_0 x + c.c.}], \quad (2.1)$$

where k_c and k_0 are the critical wave numbers associated with each instability. The amplitudes $A(X, T)$, $B(X, T)$, and $R(X, T)$ depend on the slow variables $X = \epsilon^{1/2}x$ and $T = \epsilon^{-1}t$, where ϵ is the reduced distance to one of the instability thresholds, say, the Hopf instability threshold [$\epsilon = (r - r_h)/r_h$, where r is the bifurcation parameter and r_h its critical value at the Hopf bifurcation]. The structure of their evolution equations may easily be obtained on using the symmetries of the problem and correspond to the coupled Ginzburg-Landau equations

$$\begin{aligned} \partial_T A &= V \partial_X A + \epsilon A + (1 + i\alpha) \partial_X^2 A - (1 + i\beta) |A|^2 A \\ &\quad - \gamma (1 + i\delta) |B|^2 A - u(1 + i\nu) |R|^2 A, \\ \partial_T B &= -V \partial_X B + \epsilon B + (1 + i\alpha) \partial_X^2 B - (1 + i\beta) |B|^2 B \\ &\quad - \gamma (1 + i\delta) |A|^2 B - u(1 + i\nu) |R|^2 B, \\ \tau \partial_T R &= (\epsilon - \epsilon_s) R + \xi_0^2 \partial_X^2 R - |R|^2 R \\ &\quad - w(1 + i\zeta) (|A|^2 + |B|^2) R, \end{aligned} \quad (2.2)$$

where $\epsilon_s = (r_s - r_h)/r_h$ is positive when the oscillatory instability is the first to appear on increasing the bifurcation parameter, which is the case we will consider here. ξ_0^2 is related to dispersive effects; γ and δ are the cross-coupling coefficients between oscillatory modes (I will consider $-1 < \gamma$ in order to ensure supercritical bifurcations); u , ν , w , and ζ are the cross-coupling coefficients between oscillatory and steady modes.

The evolution equations for the amplitudes A and B in the absence of interactions with stationary modes have been derived and studied in different contexts [4, 19–21, 13, 22] and it

is now well known that it is the nonlinear cross-coupling term between both amplitudes that determines if the stable patterns correspond to traveling (strong cross-coupling) or standing (weak cross-coupling) waves. Their generalization to the codimension-two problem has been studied in the framework of Rayleigh-Bénard convection in binary fluids [23, 5], where the bifurcation parameter is the Rayleigh number and the wave cross-coupling term γ is larger than one and favors traveling waves. Up to now, they have not been studied for low wave cross couplings ($\gamma < 1$), which favor standing waves. This is the case of viscoelastic convection, where the amplitude equations have been calculated for non-interacting oscillatory and stationary instabilities only [6]. Hence the coefficients $u(1 + i\nu)$ and $w(1 + i\zeta)$ are not known yet. I will nevertheless study these equations for $\gamma < 1$ and arbitrary cross-coupling coefficients $u(1 + i\nu)$ and $w(1 + i\zeta)$ in order to assess the possible behavior of the solutions of these equations. The application of the results to viscoelastic convection should improve the qualitative understanding of pattern formation in polymeric solutions and provide useful hints for the interpretation of experimental results [24].

III. STABILITY OF THE GROUND STATES

In order to determine the patterns that may be selected by the dynamics (2.2), one has to analyze the stability of the different steady-state solutions and, in the first place, of the trivial conduction state. Since Eqs. (2.2) correspond to supercritical bifurcations and thus to stabilizing nonlinearities, this study may be performed through a linear stability analysis.

A. Stability of the conduction state

On linearizing Eqs. (2.2) around the trivial solution $A(X, T) = B(X, T) = R(X, T) = 0$, the complex growth rates of disturbances of wave number κ satisfy the dispersion relations

$$\begin{aligned} \omega_A &= KV + \epsilon + (1 + i\alpha)K^2, \\ \omega_B &= -KV + \epsilon + (1 + i\alpha)K^2, \quad K = k + iq \\ \omega_R &= \frac{1}{\tau} [(\epsilon - \epsilon_s) + \xi_0^2 K^2] \end{aligned} \quad (3.1)$$

and the growth rates of such perturbations are given by $\text{Re} \omega(K)$. Using the method of steepest descent, the long-time behavior of the system along a ray defined by fixed X/T , i.e., in a frame moving with a velocity $V_0 = X/T$, is governed by the saddle point defined by

$$\text{Re} \left(\frac{d\omega}{dK} \right) \Big|_{K_0} = 0, \quad \text{Im} \left(\frac{d\omega}{dK} \right) \Big|_{K_0} = V_0. \quad (3.2)$$

Since absolute instability occurs when perturbations grow at fixed locations, one has to consider the growth rate of modes evolving with zero group velocity, which are defined by

$$\text{Re} \left(\frac{d\omega}{dK} \right) = \text{Im} \left(\frac{d\omega}{dK} \right) = 0. \quad (3.3)$$

These conditions define the wave number

$$q_{A(B)} = -\alpha k_{A(B)}, \quad q_R = k_R = 0, \quad k_{A(B)} = \mp \frac{V}{2(1+\alpha^2)}. \quad (3.4)$$

The real part of ω , which determines the growth rate λ of these modes, is then

$$\lambda_{A(B)} = \text{Re}(\omega_{A(B)}) = \epsilon - \frac{V^2}{4(1+\alpha^2)},$$

$$\lambda_R = \text{Re}(\omega_R) = \epsilon - \epsilon_s. \quad (3.5)$$

Therefore, the trivial conduction state is absolutely unstable if $\lambda > 0$. As already shown in [9], this condition determines a critical line in the parameter space, which can be expressed for the group velocity V or the control parameter ϵ as

$$V_c = 2\sqrt{\epsilon(1+\alpha^2)} \quad \text{or} \quad \epsilon_c = \frac{V^2}{4(1+\alpha^2)}. \quad (3.6)$$

Hence, for $0 < \epsilon < \epsilon_c$, the conduction state is convectively unstable towards wavy modes and wave patterns are unable to develop in the absence of noise. For $\epsilon > \epsilon_c$, wave patterns may grow and are sustained by the dynamics, even in the absence of noise. On the other hand, for $0 < \epsilon < \epsilon_s$ the conduction state is stable versus stationary modes and unstable for $\epsilon_s < \epsilon$. Hence, for $\epsilon > \epsilon_c$ and $\epsilon > \epsilon_s$ both types of modes may start growing, but it is of course their nonlinear interactions that will determine the resulting patterns and their stability. Let me then consider the different possibilities, which are pure wave patterns, pure roll patterns, and mixed states involving rolls and wave patterns. I will consider here uniform amplitude solutions corresponding to spatiotemporal patterns with critical wave numbers. The stability of modulated or wave solutions will be considered later on.

B. Stability of pure wave patterns

1. Traveling waves

One class of nontrivial steady states of the dynamical system (2.2) corresponds pure critical traveling-wave solutions $A(X, T)_0 = \sqrt{\epsilon} \exp -i(\beta \epsilon T + \phi)$, $B(X, T) = R(X, T) = 0$ or $B_0(X, T) = \sqrt{\epsilon} \exp -i(\beta \epsilon T + \phi)$, $A(X, T) = R(X, T) = 0$, where ϕ is an arbitrary phase. One may consider the first family without loss of generality and, in order to study its linear stability, one has to look for solutions in the form $A(X, T) = (\sqrt{\epsilon} + a) \exp -i\beta \epsilon T$, $B(X, T) = b$ and compute the eigenvalues of the linearized evolution equations for a , b , and their complex conjugates \bar{a} and \bar{b} . The real parts of the eigenvalues of the Fourier transform of a are well known (see, for example, [25]) and read

$$\text{Re} \omega_{|a|} = -2\epsilon - (1 - \alpha\beta)q^2 + \dots,$$

$$\text{Re} \omega_{\phi} = -(1 + \alpha\beta)q^2 - \frac{\alpha^2(1 + \beta^2)}{2\epsilon}q^4 + \dots \quad (3.7)$$

The first one is always negative, but the second may become positive and the system may experience a Benjamin-Feir in-

stability when $1 + \alpha\beta$ is negative [26,27]. In the following, we will consider systems where α and β are sufficiently small and positive such that $1 + \alpha\beta > 0$.

The only remaining instability mechanism may then result from the growth of B . Effectively, the linearized evolution equations for b or \bar{b} give the growth rate

$$\omega_B = \epsilon(1 - \gamma) - i\epsilon\gamma\delta - K_V + (1 + i\alpha)K^2. \quad (3.8)$$

As in Sec. III A, the conditions (3.3) and (3.4) determine K . The stability of the solution $[\sqrt{\epsilon} \exp -i(\beta \epsilon T + \phi), 0, 0]$ is determined by the growth rates $\lambda_j = \text{Re}(\omega_j)$ ($j = A, B, R$). Since ω_A is negative, we get the following condition for absolute stability of the pure traveling-wave states:

$$\lambda_B = \text{Re}(\omega_B) = \epsilon(1 - \gamma) - \frac{V^2}{4(1 + \alpha^2)} < 0,$$

$$\lambda_R = \text{Re}(\omega_R) = \epsilon(1 - w) - \epsilon_s < 0. \quad (3.9)$$

Hence, for $\gamma > 1$ and $w > 1$, pure traveling waves are stable, while they may become unstable for $\gamma < 1$ and/or $w < 1$. For $w < 1$, traveling waves are stable for $0 < \epsilon < \epsilon_s/(1 - w)$ and become unstable versus spatial modulations for $\epsilon > \epsilon_s/(1 - w)$. For $-1 < \gamma < 1$, one has to distinguish between the following cases.

(i) $w > 1$. Stationary spatial modulations decay and pure traveling waves are thus convectively unstable, but absolutely stable versus counterpropagating wavy modes for $0 < \epsilon < \epsilon'_c = \epsilon_c/(1 - \gamma)$ and absolutely unstable for $\epsilon'_c < \epsilon$. The corresponding critical group velocity is $V'_c = V_c \sqrt{1 - \gamma}$. As a result, on increasing the bifurcation parameter in deterministic systems with $0 < \gamma < 1$, traveling waves should be expected for $\epsilon_c < \epsilon < \epsilon'_c$, as shown in Ref. [18]. However, when $\gamma < 0$, which is the case in viscoelastic convection [6], $\epsilon'_c < \epsilon_c$. Hence, in deterministic dynamics, a traveling-wave state cannot be obtained, in ramp experiments, from the trivial conduction state.

(ii) $w < 1$. The absolute and convective stability properties of pure traveling waves versus counterpropagating wavy modes remain unchanged, but they are unstable versus stationary spatial modulations for $\epsilon > \epsilon_s/(1 - w)$. Pure traveling waves are thus only convectively unstable for $\epsilon < \min[\epsilon'_c, \epsilon_s/(1 - w)]$. Hence, for $0 < \gamma < 1$, they may only be expected when $\epsilon_c < \epsilon_s/(1 - w)$ for $\epsilon_c < \epsilon < \min[\epsilon'_c, \epsilon_s/(1 - w)]$, while for $\gamma < 0$, they still cannot be obtained from the trivial conduction state.

2. Stability of standing waves

A second class of nontrivial steady states of the dynamical system (2.2) corresponds to the pure critical standing-wave solutions $A_s(X, T) = \sqrt{\epsilon/(1 + \gamma)} \exp -i[(\beta + \gamma\delta)/(1 + \gamma)\epsilon T + \phi]$, $B_s(X, T) = \sqrt{\epsilon/(1 + \gamma)} \exp -i[(\beta + \gamma\delta)/(1 + \gamma)\epsilon T + \psi]$, and $R(X, T) = 0$, where ϕ and ψ are arbitrary phases. For $\gamma > 1$, standing waves are known to be unstable. For $\gamma < 1$, standing waves are stable versus perturbations in A and B , provided $1 + \alpha(\beta - \gamma^2\delta)/(1 - \gamma^2) > 0$ [19] (which reduces to the habitual Benjamin-Feir criterion $1 + \alpha\beta > 0$ in the special case where $\delta = \beta$ [28]). I will consider here that these conditions are satisfied, as it is usually

the case for convection in Oldroyd-*B* viscoelastic fluids [7], which is a typical example of system where $\gamma < 1$. Note that the results obtained below are also valid for noncritical standing-wave solutions in their phase stability domain (the phase stability condition being derived in [7]). Outside this domain, one needs to study the convective absolute stability of the corresponding patterns, an aspect that will be analyzed later on. For the time being, let us consider only critical standing waves that are stable versus wavy mode perturbations.

The full stability analysis also requires one to study the growth rate of spatial disturbances in R around the state $(A_s, B_s, 0)$, which is given by

$$\lambda_R = \text{Re}(\omega_R) = \epsilon \left(1 - \frac{2w}{1+\gamma} \right) - \epsilon_s. \tag{3.10}$$

In these conditions, critical standing waves are thus stable for any $\epsilon > 0$ if $2w > 1 + \gamma$ and for $0 < \epsilon < \epsilon_s [(1 + \gamma)/(1 + \gamma - 2w)]$ if $2w < 1 + \gamma$.

C. Stability of steady rolls

The linear growth rates of the wavy mode perturbations around the pure critical roll state $(0, 0, R_0 = \sqrt{\epsilon - \epsilon_s} \exp i\phi)$ that may exist for $\epsilon - \epsilon_s$ are given by

$$\omega_A = KV + \epsilon + (1 + i\alpha)K^2 - u(1 + iv)(\epsilon - \epsilon_s),$$

$$\omega_B = -KV + \epsilon + (1 + i\alpha)K^2 - u(1 + iv)(\epsilon - \epsilon_s),$$

$$K = k + iq. \tag{3.11}$$

The standard analysis shows that this state is stable for

$$\epsilon(1 - u) + u\epsilon_s < 0. \tag{3.12}$$

It is convectively unstable for

$$\epsilon(1 - u) + u\epsilon_s > 0 \tag{3.13}$$

and absolutely unstable for

$$\epsilon(1 - u) - (\epsilon_c - u\epsilon_s) > 0. \tag{3.14}$$

Hence, for $u < 1$, pure rolls are absolutely unstable for any $\epsilon > \epsilon_s$ when $\epsilon_c < \epsilon_s$, while for $\epsilon_c > \epsilon_s$, they are convectively unstable and absolutely stable for $\epsilon_s < \epsilon < (\epsilon_c - u\epsilon_s)/(1 - u)$ and absolutely unstable for $(\epsilon_c - u\epsilon_s)/(1 - u) < \epsilon$. On the other hand, for $u > 1$ and $\epsilon_c > \epsilon_s$, they are convectively unstable and absolutely stable for any $\epsilon_s < \epsilon < (u\epsilon_s)/(u - 1)$, while for $\epsilon_c < \epsilon_s$, they are absolutely unstable for $\epsilon_s < \epsilon < (u\epsilon_s - \epsilon_c)/(u - 1)$ and convectively unstable for $(u\epsilon_s - \epsilon_c)/(u - 1) < \epsilon < u\epsilon_s/(u - 1)$. In both cases, they are convectively stable for $u\epsilon_s/(u - 1) < \epsilon$.

D. Stability of mixed states

The mixed states may be of two types, which result from superpositions of rolls and traveling wave states or rolls and standing wave states.

1. Mixed traveling waves and roll states

These states are asymptotic solutions of the equations

$$\begin{aligned} \partial_T A &= V \partial_X A + \epsilon A + (1 + i\alpha) \partial_X^2 A - (1 + i\beta) |A|^2 A \\ &\quad - u(1 + iv) |R|^2 A, \\ \tau \partial_T R &= (\epsilon - \epsilon_s) R + \xi_0^2 \partial_X^2 R - |R|^2 R \\ &\quad - w(1 + i\zeta) |A|^2 R, \end{aligned} \tag{3.15}$$

with $B = 0$ (or the symmetric states where A and B are exchanged). Their uniform solutions may be written as $A = |A_m| e^{i\phi_{A_m}}$ and $R = |R_m| e^{i\phi_{R_m}}$ and satisfy

$$\begin{aligned} \epsilon - |A_m|^2 - u |R_m|^2 &= 0, \\ \epsilon - \epsilon_s - |R_m|^2 - w |A_m|^2 &= 0, \\ \phi_{A_m} &= -(\beta |A_m|^2 + uv |R_m|^2) t, \\ \phi_{R_m} &= -w \zeta |A_m|^2 t. \end{aligned} \tag{3.16}$$

As a result, one has

$$|A_m|^2 = \frac{\epsilon(1 - u) + u\epsilon_s}{1 - uw}, \quad |R_m|^2 = \frac{\epsilon(1 - w) - \epsilon_s}{1 - uw}. \tag{3.17}$$

The positivity of the norms require that $uw < 1$, $\epsilon(1 - u) + u\epsilon_s > 0$, and $\epsilon(1 - w) - \epsilon_s > 0$. Hence these solutions never exist for $w > 1$, while for $w < 1$, they exist for all $\epsilon > \epsilon_s/(1 - w)$ if $u < 1$ and for $\epsilon_s/(1 - w) < \epsilon < u\epsilon_s/(u - 1)$ for $1 < u < 1/w$.

Besides their stability versus perturbations in A and R , which has to be analyzed within the system (3.15), one also has to determine their stability versus perturbations in B , around $B = 0$, which has the linear dispersion relation

$$\begin{aligned} \omega_B &= -KV + (1 + i\alpha)K^2 + \epsilon - \gamma(1 + i\delta) \frac{\epsilon(1 - u) + u\epsilon_s}{1 - uw} \\ &\quad - u(1 + iv) \frac{\epsilon(1 - w) - \epsilon_s}{1 - uw}. \end{aligned} \tag{3.18}$$

The growth rate of the modes that evolve with zero group velocity is thus

$$\begin{aligned} \lambda_B &= \epsilon \frac{(1 - \gamma)(1 - u) - uw}{1 - uw} + \epsilon_s \frac{u(1 - \gamma)}{1 - uw} - \frac{V^2}{4(1 + \alpha^2)} \\ &= (1 - \gamma) \frac{\epsilon(1 - u) + u\epsilon_s - \epsilon'_c(1 - uw)}{1 - uw}. \end{aligned} \tag{3.19}$$

Hence, when $\gamma > 1$, this state is stable, while for $\gamma < 1$, it is absolutely unstable, except for

$$\frac{\epsilon_s}{1 - w} < \epsilon < \frac{\epsilon'_c(1 - uw) - u\epsilon_s}{1 - u} \tag{3.20}$$

when $u < 1$ and for

$$\frac{u\epsilon_s - \epsilon'_c(1-uw)}{u-1} < \epsilon < \frac{u\epsilon_s}{u-1} \tag{3.21}$$

when $1 < u < 1/w$.

2. Mixed standing waves and roll states

These states are asymptotic solutions of the complete equations (2.2), where $A, B, R \neq 0$. The uniform solutions may be written as $A = |A_m|e^{i\phi_{A_m}}$, $B = |B_m|e^{i\phi_{B_m}}$, and $R = |R_m|e^{i\phi_{R_m}}$ and satisfy

$$\begin{aligned} \epsilon - |A_m|^2 - \gamma|B_m|^2 - u|R_m|^2 &= 0, \\ \epsilon - |B_m|^2 - \gamma|A_m|^2 - u|R_m|^2 &= 0, \\ \epsilon - \epsilon_s - |R_m|^2 - w(|A_m|^2 + |B_m|^2) &= 0, \\ \phi_{A_m} &= -(\beta|A_m|^2 + \gamma\delta|B_m|^2 + uv|R_m|^2)t, \\ \phi_{B_m} &= -(\beta|B_m|^2 + \gamma\delta|A_m|^2 + uv|R_m|^2)t, \\ \phi_{R_m} &= -w\zeta(|A_m|^2 + |B_m|^2)t, \end{aligned} \tag{3.22}$$

which gives

$$\begin{aligned} |A_m|^2 = |B_m|^2 &= \frac{\epsilon(1-u) + u\epsilon_s}{1 + \gamma - 2uw}, \\ |R_m|^2 &= \frac{\epsilon(1 + \gamma - 2w) - (1 + \gamma)\epsilon_s}{1 + \gamma - 2uw}. \end{aligned} \tag{3.23}$$

Hence, such states do not exist for $w > (1 + \gamma)/2$, while for $w < (1 + \gamma)/2$ they exist for $(1 + \gamma)\epsilon_s / (1 + \gamma - 2w) < \epsilon$ when $u < 1$ and for $\epsilon_w = (1 + \gamma)\epsilon_s / (1 + \gamma - 2w) < \epsilon < u\epsilon_s / (u - 1) = \epsilon_u$ when $1 < u < (1 + \gamma)/2w$. For $\gamma > 1$ these states are unstable, while for $\gamma < 1$ they are amplitude stable, but could be phase unstable, according to the value of the imaginary parts of the kinetic coefficients. In the following, I will consider them as stable, which is the case when the imaginary parts of the kinetic coefficients are sufficiently small.

IV. PATTERN SELECTION IN DETERMINISTIC SYSTEMS

In this discussion, I will consider separately the case where $\gamma > 1$, which favors traveling waves, and the case where γ varies in the range $-1 < \gamma < 1$, which implies supercritical bifurcations and preferred standing-wave solutions.

When $\gamma > 1$, in the absence of group velocity, traveling waves (TWs) may develop for any $\epsilon > 0$. For $w > 1$, they remain stable versus spatial modulations, although roll patterns may also develop in the range $\epsilon > u\epsilon_s / (u - 1)$, when $u > 1$. For $w < 1$, TW states lose stability versus spatial modulations at $\epsilon = \epsilon_s / (1 - w)$, where they bifurcate to rolls when $uw > 1$ or mixed modes when $uw < 1$.

In the presence of group velocity, TWs may only be sustained by the dynamics for $\epsilon > \epsilon_c$. For $w > 1$, they remain stable versus spatial modulations for all $\epsilon > \epsilon_c$, while rolls are stable in the range $\epsilon_s < \epsilon < (\epsilon_c - u\epsilon_s) / (1 - u)$ when $u < 1$ and for $\epsilon_s < \epsilon$ (if $\epsilon_s < \epsilon_c$) or $(u\epsilon_s - \epsilon_c) / (1 - u) < \epsilon$ (if

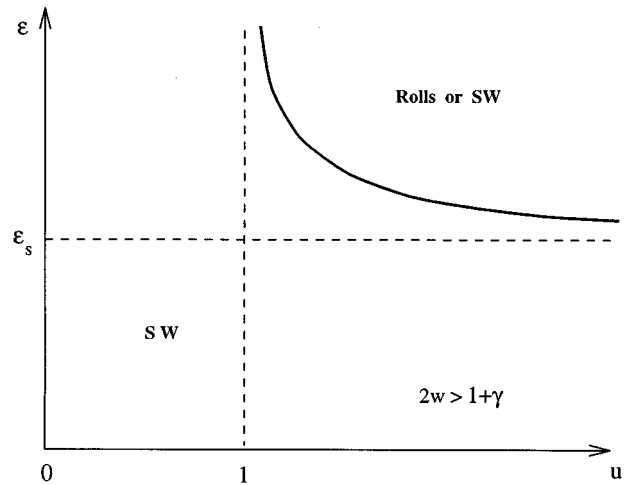


FIG. 1. Schematic phase diagram associated with the dynamical system (2.2), in the (ϵ, u) plane, for $V=0$, $\gamma < 0$, $\alpha=0.1$, $\beta = \delta=0.15$, and $v = \zeta=0$ when $w > (1 + \gamma)/2$.

$\epsilon_s > \epsilon_c$) when $u > 1$. For $w < 1$, TW states again lose stability versus spatial modulations at $\epsilon = \epsilon_s / (1 - w)$, where they bifurcate to rolls when $uw > 1$ or mixed modes when $uw < 1$. They are thus stable in the range $\epsilon_c < \epsilon < \epsilon_s / (1 - w)$.

Let me consider now weak cross couplings such that $-1 < \gamma < 1$. When $w > (1 + \gamma)/2$, standing waves may develop, in this case, for any $\epsilon > 0$ in the absence of group velocity (bistability with steady rolls may occur for $\epsilon > \epsilon_s [u / (u - 1)]$ if $u > 1$). For $w < (1 + \gamma)/2$, however, standing waves (SWs) are stable up to $\epsilon = \epsilon_s [(1 + \gamma) / (1 + \gamma - 2w)]$, where it bifurcates to mixed modes if $u < (1 + \gamma) / 2w$ or to rolls if $u > (1 + \gamma) / 2w$. In the range $1 < u < (1 + \gamma) / 2w$, the mixed modes state bifurcates to steady rolls at $\epsilon = \epsilon_s [u / (u - 1)]$. The corresponding phase diagrams are represented in Figs. 1 and 2.

The presence of group velocity may strongly modify this picture since the conducting state is convectively unstable but absolutely stable for positive values of ϵ . For the sake of

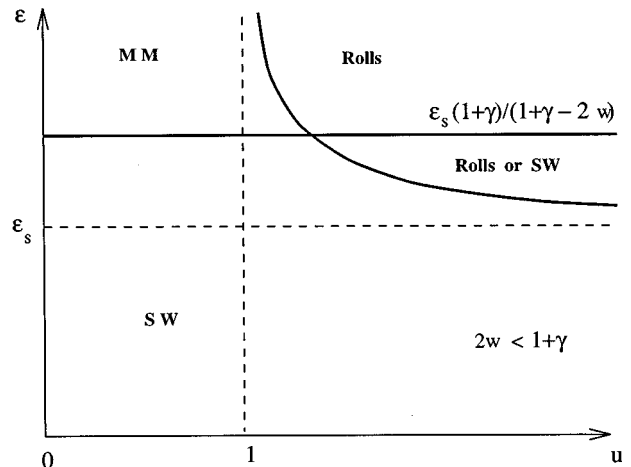


FIG. 2. Phase diagram associated with the dynamical system (2.2) for $V=0$, $\gamma < 0$, $\alpha=0.1$, $\beta = \delta=0.15$, and $v = \zeta=0$ when $w < (1 + \gamma)/2$.

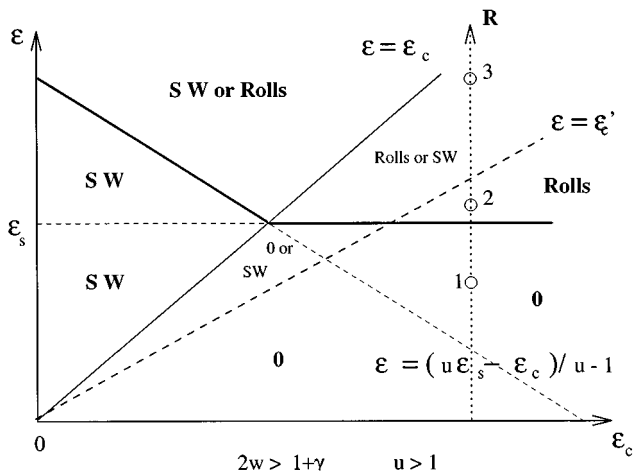


FIG. 3. Schematic phase diagram associated with the dynamical system (2.2) with nonvanishing group velocity $V \neq 0$, in the (ϵ, ϵ_c) plane, for $\gamma < 0$, $\alpha = 0.1$, $\beta = \delta = 0.15$, and $v = \zeta = 0$ when $w > (1 + \gamma)/2$ and $u > 1$.

simplicity, I will consider $\gamma < 0$, which implies that TW states become absolutely unstable before the conduction state, which then bifurcates directly to SWs or roll states. Let me consider first ramp experiments in dynamical systems where $w > (1 + \gamma)/2$, which prohibits the existence of mixed states. In such systems, one has to distinguish further between the $u < 1$ and $u > 1$ cases, with $\epsilon_c < \epsilon_s$ or $\epsilon_s < \epsilon_c$. When $w > (1 + \gamma)/2$ and $\epsilon_c < \epsilon_s$, the trivial conduction state remains convectively unstable up to $\epsilon = \epsilon_c$, where it bifurcates to standing waves (although steady rolls could in principle appear for any $\epsilon > \epsilon_s$, they can only be sustained by the dynamics for $u > 1$ in the range $\epsilon_s[u/(u-1)] < \epsilon$, while they are absolutely unstable for $u < 1$). In quench experiments, standing waves may appear as soon as $\epsilon'_c < \epsilon$.

On the contrary, when $w > (1 + \gamma)/2$ and $\epsilon_c > \epsilon_s$, the trivial conduction state remains convectively unstable up to $\epsilon = \epsilon_s$ where it bifurcates to steady rolls. For $u < 1$, these rolls are convectively unstable up to $\epsilon = (\epsilon_c - u\epsilon_s)/(1 - u)$, where they become absolutely unstable and bifurcate to standing waves. Since standing waves are stable as soon as $\epsilon > \epsilon_c$, the system is bistable in the range $\epsilon_c < \epsilon < (\epsilon_c - u\epsilon_s)/(1 - u)$. For $u > 1$ rolls are convectively unstable for $\epsilon_s < \epsilon < \epsilon_s[u/(u-1)]$ and stable for $\epsilon_s[u/(u-1)] < \epsilon$. The corresponding phase diagrams are represented in Figs. 3 and 4.

For $w < (1 + \gamma)/2$, the previous results are modified as follows.

(i) For $\epsilon_c < \epsilon_s$ and $u < 1$, the trivial conduction state is convectively unstable up to $\epsilon = \epsilon_c$, where it bifurcates to standing waves. These standing waves are stable up to $\epsilon = \epsilon_s[(1 + \gamma)/(1 + \gamma - 2w)]$, where they bifurcate to a mixed standing-wave-roll state.

(ii) For $\epsilon_c < \epsilon_s$ and $1 < u < (1 + \gamma)/2w$, the trivial conduction state is convectively unstable up to $\epsilon = \epsilon_c$, where it bifurcates to standing waves. These standing waves are stable up to $\epsilon = \epsilon_s[(1 + \gamma)/(1 + \gamma - 2w)]$, where they bifurcate to a mixed standing-wave-roll state. This mixed-mode state becomes unstable at $\epsilon = \epsilon_s[u/(u-1)]$, where it bifurcates to steady rolls.

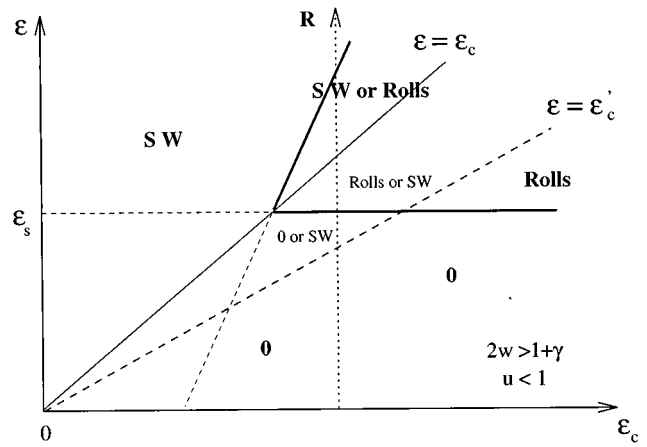


FIG. 4. Schematic phase diagram associated with the dynamical system (2.2) with nonvanishing group velocity $V \neq 0$, in the (ϵ, ϵ_c) plane, for $\gamma < 0$, $\alpha = 0.1$, $\beta = \delta = 0.15$, and $v = \zeta = 0$ when $w > (1 + \gamma)/2$ and $u < 1$.

(iii) For $\epsilon_c < \epsilon_s$ and $(1 + \gamma)/2w < u$, the trivial conduction state is also convectively unstable up to $\epsilon = \epsilon_c$, where it bifurcates to standing waves. These standing waves are stable up to $\epsilon = \epsilon_s[(1 + \gamma)/(1 + \gamma - 2w)]$, where they bifurcate directly to steady rolls, with no intermediate mixed-mode state.

(iv) For $\epsilon_s < \epsilon_c$ and $u < 1$, the trivial conduction state is convectively unstable up to $\epsilon = \epsilon_s$, where it bifurcates to steady rolls. These rolls are stable up to $\epsilon = (\epsilon_c - u\epsilon_s)/(1 - u)$, where they bifurcate to the mixed standing-wave-rolls state.

(v) For $\epsilon_s < \epsilon_c$ and $1 < u$, the trivial conduction state is convectively unstable up to $\epsilon = \epsilon_s$, where it bifurcates to steady rolls. These rolls remain stable for increasing ϵ . The corresponding phase diagrams are represented in Figs. 5 and 6.

When $0 < \gamma < 1$, the only qualitative modification to these results is that, on increasing the bifurcation parameter, TW states may appear between the conduction state and standing waves, as shown, for example, in Fig. 7.

V. THE EFFECT OF NOISE

It may be expected, as in other cases of convective and absolute instability, that noise could play an important role here in sustaining spatiotemporal patterns that should otherwise be convected away by mean flow effects. In the absence of stationary instability, spatially distributed noise should sustain standing or traveling waves, according to the value of γ , in the range $0 < \epsilon < \epsilon_c$, while these waves are intrinsically sustained by the dynamics for $\epsilon_c < \epsilon$. On removing the noise in systems where $\gamma < 0$ and $\epsilon'_c < \epsilon_c$, the system relaxes to the conducting state for $0 < \epsilon < \epsilon_c$ and to traveling waves for $\epsilon'_c < \epsilon < \epsilon_c$, as shown in [13].

When the oscillatory instability is close to the stationary one, leading to possible interactions between steady and wavy modes, the situation may be more intricate. In particular, the pattern selection obtained in the preceding section should be modified as follows. On the one hand, for $\epsilon > \epsilon_c$, the deterministic pattern selection should not be af-

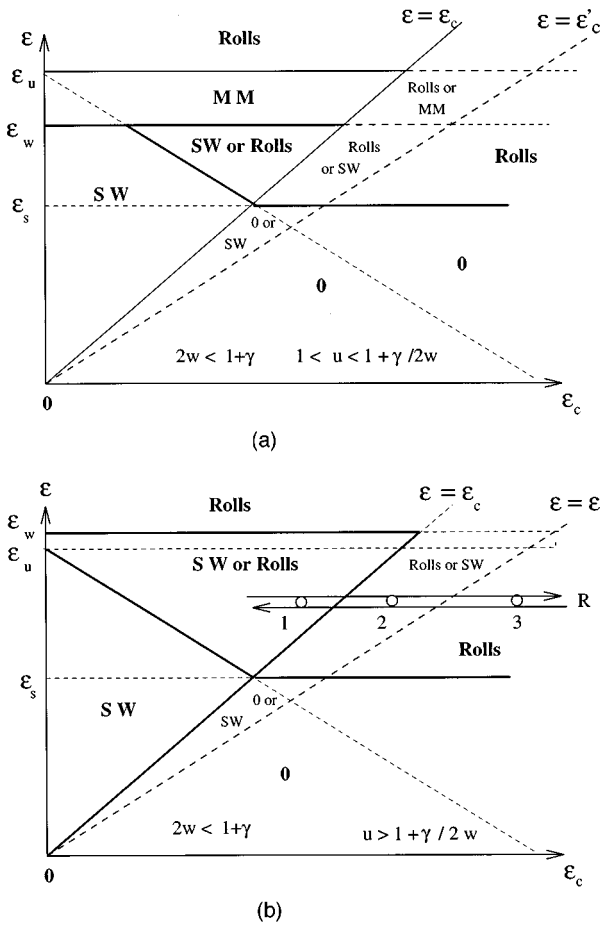


FIG. 5. Schematic phase diagram associated with the dynamical system (2.2) with nonvanishing group velocity $V \neq 0$, in the (ϵ, ϵ_c) plane, for $\gamma < 0$, $\alpha = 0.1$, $\beta = \delta = 0.15$, and $v = \zeta = 0$ when $w < (1 + \gamma)/2$ and (a) $(1 + \gamma)/2w < u$ and (b) $1 < u < (1 + \gamma)/2w$.

ected by the presence of noise since all the possible patterns are intrinsically sustained by the dynamics. On the other hand, standing or traveling waves should be sustained by spatially distributed noise for $0 < \epsilon < \epsilon_c$ in ramp experiments

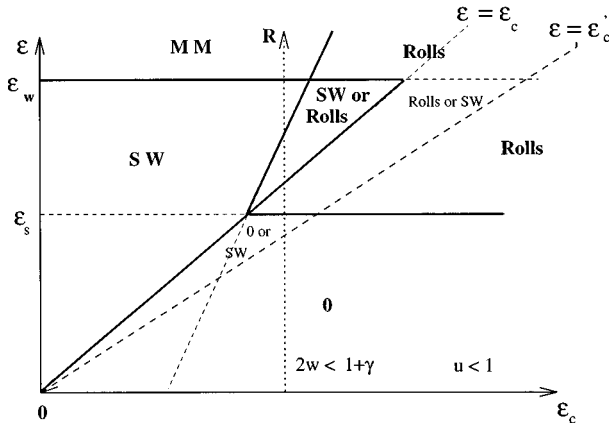


FIG. 6. Schematic phase diagram associated with the dynamical system (2.2) with nonvanishing group velocity $V \neq 0$, in the (ϵ, ϵ_c) plane, for $\gamma < 0$, $\alpha = 0.1$, $\beta = \delta = 0.15$, and $v = \zeta = 0$ when $w < (1 + \gamma)/2$ and $u < 1$.

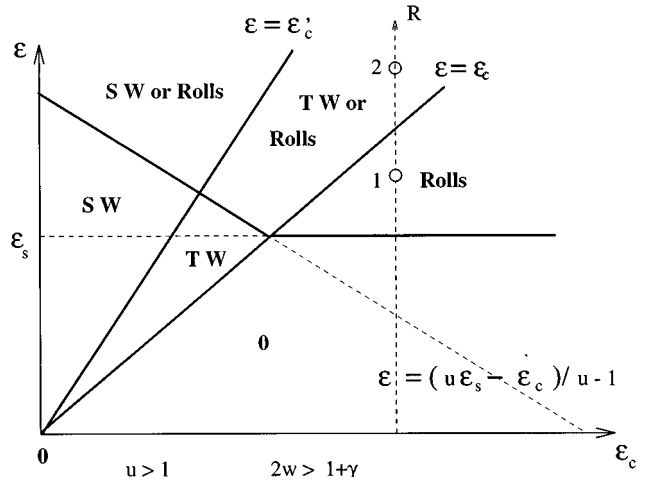


FIG. 7. Schematic phase diagram associated with the dynamical system (2.2) with nonvanishing group velocity $V \neq 0$, in the (ϵ, ϵ_c) plane, for $\gamma > 0$, $\alpha = 0.1$, $\beta = \delta = 0.15$, and $v = \zeta = 0$ when $w > (1 + \gamma)/2$ and $u > 1$.

starting from the trivial conducting state. For quench experiments in the range $\epsilon_s < \epsilon < \epsilon_c$, a competition may arise between noise sustained wave patterns and dynamically sustained roll patterns, which needs to be studied numerically, as shown in Sec. VI. On noise removal, interesting situations may occur in systems where $\epsilon_s < \epsilon'_c < \epsilon_c$ since the standing waves should relax to traveling waves for $\epsilon'_c < \epsilon < \epsilon_c$, to steady rolls for $\epsilon_s < \epsilon < \epsilon'_c$, and to the conducting state for $0 < \epsilon < \epsilon_s$.

VI. NUMERICAL ANALYSIS

The preceding results have been confirmed by numerical tests performed with a finite difference code for a system of 200 points. The boundary conditions were $A(0) = R(0) = B_x(0) = 0$ and $A_x(200) = R(200) = B(200) = 0$. For the stochastic cases, noise intensities have been chosen between 10^{-4} and 10^{-2} . The following observations are particularly relevant.

(i) In a system where $\gamma = -0.5$, $\alpha = 0.1$, $\beta = \delta = 0.15$, $v = \zeta = 0$, $w = 0.5$, $u = 2$, and $V = 1$, the following succession of patterns is obtained in a ramp experiment (e.g., line R in Fig. 3) in a deterministic system : uniform steady state up to $\epsilon = \epsilon_s$ (e.g., point 1 on line R in Fig. 3) and rolls for $\epsilon_s < \epsilon$ (e.g., points 2 and 3 on line R in Fig. 3). In stochastic systems with spatially distributed noise, standing waves form for any $\epsilon > 0$, but, on noise removal, the system relaxes to standing waves for $\epsilon'_c < \epsilon$ (e.g., point 3 on line R in Fig. 3), to rolls for $\epsilon_s < \epsilon < \epsilon'_c$ (e.g., point 2 on line R in Fig. 3), and to the trivial state for $\epsilon < \epsilon_s$. The corresponding numerical results are presented in Figs. 8–10.

In Fig. 8, $\epsilon = 0.1$, $\epsilon_s = 0.15$, and $\epsilon'_c = 0.1666\dots$, such that $\epsilon < \epsilon_s < \epsilon'_c$. In the absence of noise, a snapshot of a wavy transient that is eliminated as the result of the convective nature of the instability of the trivial ground state is represented in addition to the standing-wave pattern obtained in the presence of a distributed white noise of intensity $I = 10^{-4}$. Note the left-right asymmetry in the behavior of the amplitudes of the underlying traveling waves near the

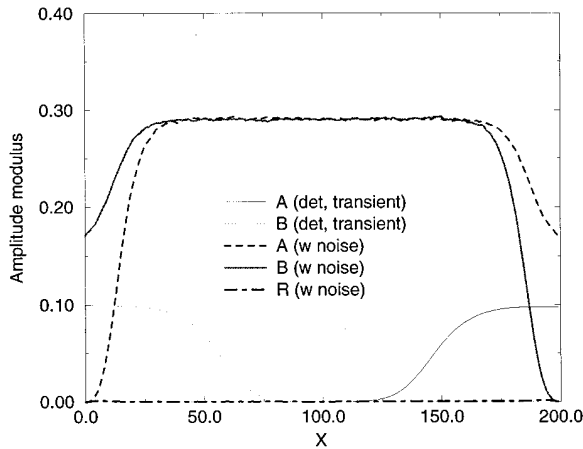


FIG. 8. Results of the numerical resolution of the dynamical system (2.2) with nonvanishing group velocity $V=1$ for $\gamma=-0.5$, $\alpha=0.1$, $\beta=\delta=0.15$, $v=\zeta=0$, $w=0.5$, $u=2$, $\epsilon=0.1$, and $\mu=\epsilon-\epsilon_s=-0.05$ (the transients disappear in the long-time limit as the result of the convective instability of the trivial steady state).

boundaries, due to the presence of the group velocity.

In Fig. 9, $\epsilon=0.15$, $\epsilon_s=0.05$, and $\epsilon'_c=0.1666\dots$, such that $\epsilon_s < \epsilon < \epsilon'_c$. Since $\epsilon_s < \epsilon$, a roll pattern is obtained in the absence of noise, while in the presence of a Gaussian white noise of amplitude $I=10^{-4}$, a standing wave pattern is obtained, similar to the one of Fig. 8, except that the boundary layer is smaller, as a consequence of the higher value of the bifurcation parameter.

In Fig. 10, $\epsilon=0.2$, $\epsilon_s=0.1$, and $\epsilon'_c=0.1666\dots$, such that $\epsilon_s < \epsilon'_c < \epsilon$, and rolls are still the selected pattern in the absence of noise. As in the preceding cases, noise sustains standing waves, which, furthermore, remain stable after noise removal (with a slight amplitude reduction though). In this case, noise not only sustains the wave pattern, but also induces a transition between rolls and standing waves.

(ii) In systems where $\gamma=0.5$, $\alpha=0.1$, $\beta=\delta=0.15$, $v=\zeta=0$, $w=1.5$, $u=2$, and $V=1$, ramp experiments (e.g.,

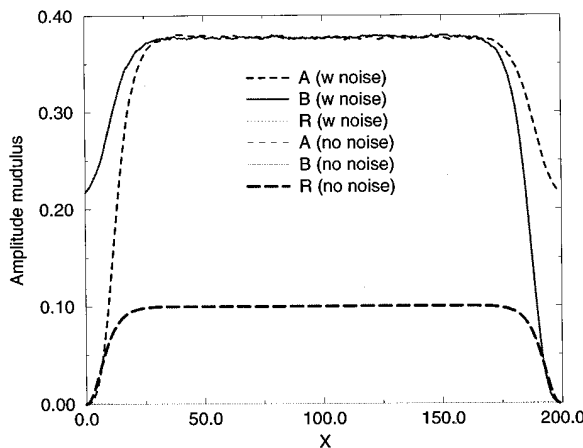


FIG. 9. Results of the numerical resolution of the dynamical system (2.2) with nonvanishing group velocity $V=1$ for $\gamma=-0.5$, $\alpha=0.1$, $\beta=\delta=0.15$, $v=\zeta=0$, $w=0.5$, $u=2$, $\epsilon=0.15$, and $\mu=\epsilon-\epsilon_s=0.1$.

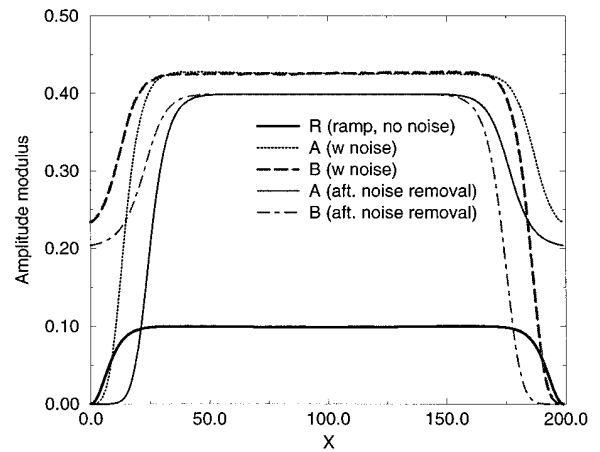


FIG. 10. Results of the numerical resolution of the dynamical system (2.2) with nonvanishing group velocity $V=1$ for $\gamma=-0.5$, $\alpha=0.1$, $\beta=\delta=0.15$, $v=\zeta=0$, $w=0.5$, $u=2$, $\epsilon=0.2$, and $\mu=\epsilon-\epsilon_s=0.1$.

line R in Fig. 7) lead to the following succession of patterns in a deterministic system: uniform steady state up to $\epsilon=\epsilon_s$ and rolls for $\epsilon_s < \epsilon$ (e.g., points 1 and 2 on line R in Fig. 7), while in stochastic systems with spatially distributed noise, standing waves form for any $0 < \epsilon$. However, after noise removal, the system relaxes to rolls for $\epsilon_s < \epsilon < \epsilon_c$ (e.g., point 1 on line R in Fig. 7) and to traveling waves for $\epsilon_c < \epsilon < \epsilon'_c$ (e.g., point 2 on line R in Fig. 7). The corresponding results are presented in Figs. 11 and 12.

In particular, in Fig. 12, $\epsilon=0.3$, $\epsilon_s=0.1$, $\epsilon_c=0.25$, and $\epsilon'_c=0.5$, such that $\epsilon_s < \epsilon_c < \epsilon < \epsilon'_c$. Hence rolls are still the selected pattern in deterministic systems and standing waves may be sustained by distributed white noise. However, since ϵ is such that the conduction state is absolutely unstable, while traveling waves are only convectively unstable, the latter are obtained after noise removal. Here also noise mediates a transition from rolls to wave patterns.

I have furthermore tested the effect of group velocity

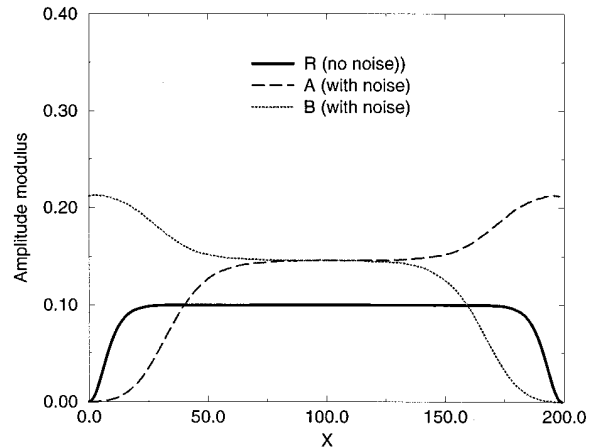


FIG. 11. Results of the numerical resolution of the dynamical system (2.2) with nonvanishing group velocity $V=1$ for $\gamma=0.5$, $\alpha=0.1$, $\beta=\delta=0.15$, $v=\zeta=0$, $w=0.5$, $u=2$, $\epsilon=0.2$, and $\mu=\epsilon-\epsilon_s=0.1$.

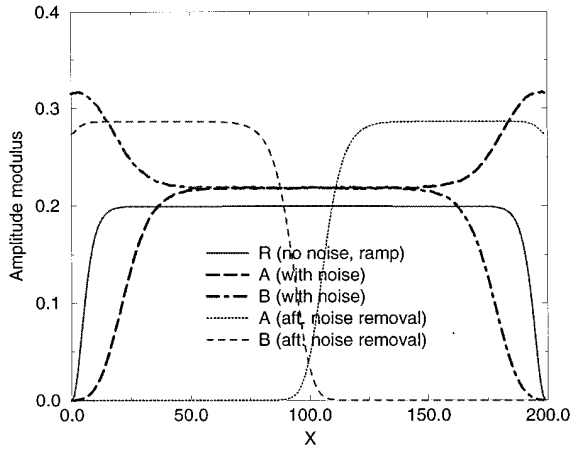


FIG. 12. Results of the numerical resolution of the dynamical system (2.2) with nonvanishing group velocity $V=1$ for $\gamma=0.5$, $\alpha=0.1$, $\beta=\delta=0.15$, $v=\zeta=0$, $w=1.5$, $u=2$, $\epsilon=0.3$, and $\mu=\epsilon-\epsilon_s=0.2$.

variations in deterministic systems where $\gamma=-0.5$, $\alpha=0.1$, $\beta=\delta=0.15$, $v=\zeta=0$, $w=0.2$, and $u=1.2$. Results are presented in Fig. 13, where it may be seen that, on increasing the group velocity from $V=0.5$ to $V=1.5$ [e.g., states 1 to 3 on line R in Fig. 5(b)], one passes from standing waves ($V=0.5$ and $V=1$) to rolls ($V=1.5$), while on decreasing the group velocity from $V=1.5$ to $V=0.5$, the system remains in the rolls state, confirming the bistability of rolls and waves patterns.

On the other hand, interesting competition phenomena may occur between noise and dynamically sustained structures. Although such a competition is difficult to quantify and requires a systematic numerical analysis, preliminary results show that the cross-coupling terms that renormalize the growth rate of the different kinds of modes could play a capital role in dynamical selection processes. For example, in a perfect codimension-2 situation ($\epsilon_s=0$), numerical results obtained for $\gamma=0.5$, $u=2$, and small imaginary parts of the kinetic coefficients strongly differ for $w < u/2$ and $w > u/2$ in the presence of noise. For example, for $w=0.8$,

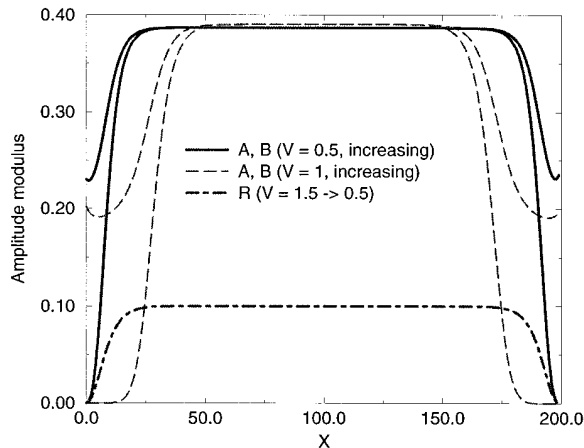


FIG. 13. Results of the numerical resolution of the dynamical system (2.2) with varying group velocities for $\gamma=-0.5$, $\alpha=0.1$, $\beta=\delta=0.15$, $v=\zeta=0$, $w=0.2$, $u=1.2$, $\epsilon=0.2$, and $\mu=\epsilon-\epsilon_s=0.1$.

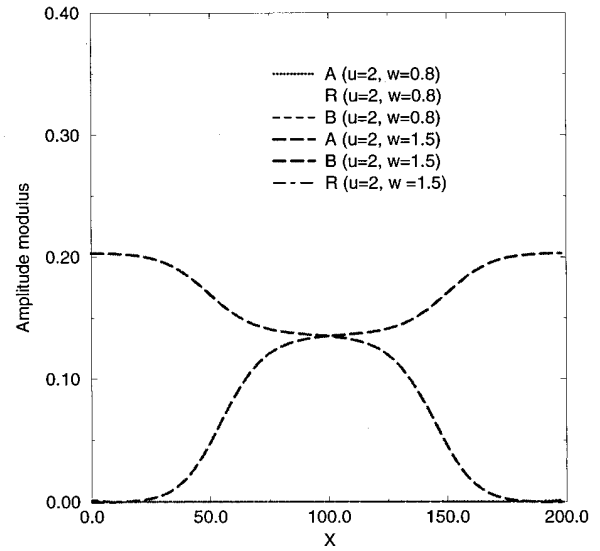


FIG. 14. Results of the numerical resolution of the dynamical system (2.2) with nonvanishing group velocity $V=1$, in the presence of spatially distributed noise of low intensity ($I=2 \times 10^{-4}$), for $\epsilon=0.2$, $\mu=\epsilon-\epsilon_s=0.2$, $\gamma=0.5$, $\alpha=0.1$, $\beta=\delta=0.03$, $v=\zeta=0.07$, $u=2$, and two different values of w ($w=0.8$ and $w=1.5$).

roll structures emerge for noise intensities $I=10^{-4}$ (Fig. 14) or $I=8 \times 10^{-3}$ (Fig. 15). However, for $w=1.5$, rolls or waves emerge at random for low noise intensities ($I=10^{-4}$) (cf. Fig. 14), while waves always emerge at higher noise intensities ($I=8 \times 10^{-4}$) (cf. Fig. 15). The numerical results also confirm that the healing length or boundary layer extension decreases for increasing noise intensity.

On the other hand, for $w=1.5$, the stability of rolls obtained in a deterministic quench has been tested versus spatially distributed noise of increasing intensity. In such an experiment, once steady rolls are obtained, all the parameters of the dynamics are kept constant, except the noise intensity, which is slowly increased. As shown in Fig. 16, rolls turned

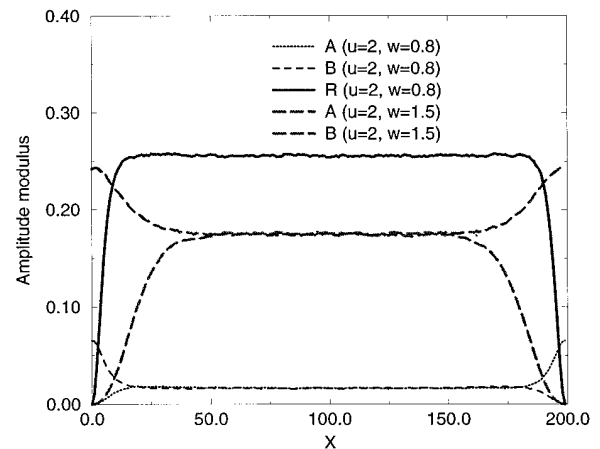


FIG. 15. Results of the numerical resolution of the dynamical system (2.2) with nonvanishing group velocity $V=1$, in the presence of spatially distributed noise of higher intensity ($I=8 \times 10^{-3}$), for $\epsilon=0.2$, $\mu=\epsilon-\epsilon_s=0.2$, $\gamma=0.5$, $\alpha=0.1$, $\beta=\delta=0.03$, $v=\zeta=0.07$, $u=2$, and two different values of w ($w=0.8$ and $w=1.5$).

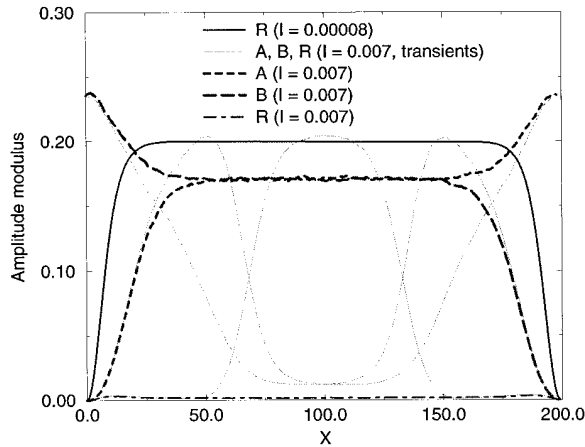


FIG. 16. Results of the numerical resolution of the dynamical system (2.2) with nonvanishing group velocity $V=1$, in the presence of spatially distributed noise of increasing intensity (I) ($\epsilon=0.2$, $\mu=\epsilon-\epsilon_s=0.2$, $\gamma=0.5$, $\alpha=0.1$, $\beta=\delta=0.03$, $v=\zeta=0.07$, $u=2$, and $w=1.5$), showing a noise-induced transition from roll to wave patterns.

out to be stable up to noise intensities of the order of 6×10^{-3} , where they bifurcate to wave patterns. These results confirm the subtle interplay between dynamic and stochastic effects on pattern selection in convectively unstable systems.

Finally, it has to be noted that the amplitude of the patterns are also noise amplified. Effectively, although the moduli $|A|^2$, $|B|^2$, and $|R|^2$ obtained numerically are found to agree with the analytical ones in deterministic systems, they are amplified in the presence of noise, as shown in Fig. 17. In this case, rolls are sustained by the dynamics and, in the absence of noise, the mean value of the modulus $\langle |R|^2 \rangle$ reaches the expected deterministic value $\epsilon = 0.2$ in the bulk. In the presence of spatially distributed noise, this value increases with noise intensity (for example, for a noise intensity of 8×10^{-3} , $|R|^2$ reaches 0.256), in agreement with the fact that the linear evolution of the mean square of the deviation of the roll amplitude around its deterministic value ($\rho=R-\sqrt{\epsilon}$) tends to an asymptotic value proportional to the noise intensity.

VII. CONCLUSION

The conclusion of the analysis performed in this paper is that the presence of group velocity and mean flows may strongly affect pattern selection and stability in systems described by coupled Ginzburg-Landau equations, especially

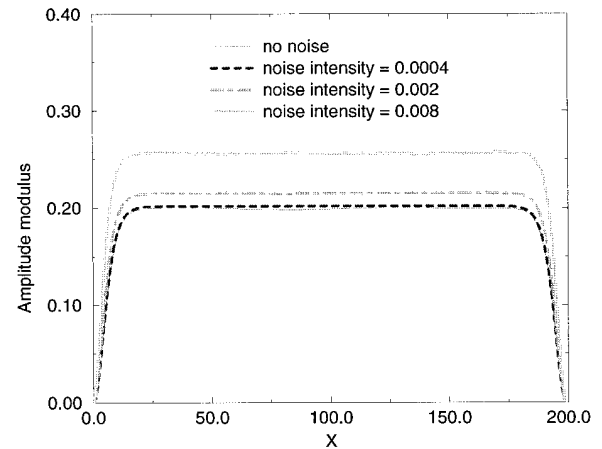


FIG. 17. Modulus of the roll amplitude $|R|^2$ obtained numerically from the dynamical system (2.2) in the presence of spatially distributed noise of increasing intensity (I) ($\epsilon=0.2$, $\mu=\epsilon-\epsilon_s=0.2$, $\gamma=0.5$, $\alpha=0.1$, $\beta=\delta=0.03$, $v=\zeta=0.07$, $u=2$, $w=0.8$, and $V=1$).

when the corresponding Hopf bifurcation is close to another instability, which leads, for example, to steady roll patterns, as in the case of binary or viscoelastic fluid convection.

When the absolute instability threshold of the trivial steady state remains below the stationary instability ($\epsilon_c < \epsilon_s$), the transition to wave patterns is only retarded by the mean flow in deterministic systems, contrary to stochastic ones where noise is able to sustain such patterns in the convectively unstable regime. In this case, pattern selection is thus not qualitatively modified by the neighboring stationary instability.

On the contrary, in deterministic systems, when $\epsilon_c > \epsilon_s$, standing waves are eliminated as an intermediate pattern between the conduction state and rolls or mixed modes, although bistability domains may exist. However, the succession of patterns that would occur in the absence of mean flow is recovered in the presence of spatially distributed noise, although interesting competition phenomena may occur between noise and dynamically sustained structures. Preliminary numerical analysis show that, in this case, pattern selection should be very sensitive to the interplay between kinetic and stochastic effects on the one hand and experimental protocols on the other.

ACKNOWLEDGMENTS

Financial assistance through a grant from the Ministerio de Education y Ciencia (DGICYT, Madrid) and through a travel grant from the Belgian National Fund for Scientific Research is gratefully acknowledged.

- [1] R. Walden, P. Kolodner, A. Passner, and C.M. Surko, *Phys. Rev. Lett.* **55**, 496 (1985).
- [2] A. Joets and R. Ribotta, in *Propagation in Systems Far from Equilibrium*, edited by J.E. Wesfreid *et al.* (Springer, New York, 1988), p. 176.
- [3] C.D. Andereck and F. Hayot, *Ordered and Turbulent Patterns*

in Taylor-Couette Flow (Plenum, New York, 1992).

- [4] M.C. Cross and P.C. Hohenberg, *Rev. Mod. Phys.* **65**, 851 (1993).
- [5] W. Schopf and W. Zimmermann, *Phys. Rev. E* **47**, 1739 (1993).
- [6] J. Martinez-Mardones, R. Tiemann, W. Zeller, and C. Perez-

- Garcia, *Int. J. Bifurcation Chaos* **4**, 1347 (1994).
- [7] J. Martinez-Mardones, R. Tiemann, D. Walgraef, and W. Zeller, *Phys. Rev. E* **54**, 1478 (1996).
- [8] P. Huerre, in *Instabilities and Nonequilibrium Structures*, edited by E. Tirapegui and D. Villarroel (Reidel, Dordrecht, 1987), p. 141.
- [9] R.J. Deissler, *J. Stat. Phys.* **40**, 376 (1985); **54**, 1459 (1989); *Physica D* **25**, 233 (1987).
- [10] H.W. Mueller, M. Luecke, and M. Kamps, *Phys. Rev. A* **45**, 3714 (1992).
- [11] P. Buechel, M. Luecke, D. Roth, and R. Schmitz, *Phys. Rev. E* **53**, 4764 (1996).
- [12] H.W. Mueller and M. Tveitereid, *Phys. Rev. Lett.* **74**, 1582 (1995).
- [13] R.J. Deissler and H.R. Brand, *Phys. Lett. A* **130**, 293 (1988).
- [14] H.R. Brand, R.J. Deissler, and G. Ahlers, *Phys. Rev. A* **43**, 4262 (1991).
- [15] K.L. Babcock, G. Ahlers, and D.S. Cannell, *Phys. Rev. E* **50**, 3670 (1994).
- [16] A. Tsameret and V. Steinberg, *Europhys. Lett.* **14**, 331 (1991); *Phys. Rev. E* **49**, 1291 (1994).
- [17] M. Luecke and A. Recktenwald, *Europhys. Lett.* **22**, 559 (1993).
- [18] M. Neufeld, D. Walgraef, and M. San Miguel, *Phys. Rev. E* **54**, 6344 (1996).
- [19] P. Coullet, S. Fauve, and E. Tirapegui, *J. Phys. (Paris) Lett.* **46**, L787 (1985).
- [20] S. Fauve, in *Instabilities and Nonequilibrium Structures* (Ref. [8]), pp. 69–88.
- [21] M. Bestehorn, R. Friedrich, and H. Haken, *Z. Phys. B* **72**, 265 (1988).
- [22] P. Coullet, T. Frisch, and F. Plaza, *Physica D* **62**, 75 (1993).
- [23] H.R. Brand, P.C. Hohenberg, and V. Steinberg, *Phys. Rev. A* **27**, 591 (1983); **30**, 2548 (1984).
- [24] P. Kolodner (unpublished).
- [25] P. Coullet, L. Gil, and J. Lega, *Physica D* **37**, 91 (1989).
- [26] T.B. Benjamin and J.E. Feir, *J. Fluid Mech.* **27**, 417 (1967).
- [27] A.C. Newell, *Lectures in Applied Mathematics*, (American Mathematical Society, Providence, RI, 1974), Vol. 15, p. 157.
- [28] M. San Miguel, *Phys. Rev. Lett.* **75**, 425 (1995).